

DRAGON: Monte Carlo generator of particle production from a fragmented fireball in ultrarelativistic nuclear collisions^{*}

Boris Tomášik

*Fakulta prírodných vied, Univerzita Mateja Bela, Tajovského 40,
97401 Banská Bystrica, Slovakia*

*Inštitút matematiky a informatiky, Univerzita Mateja Bela,
Cesta na Amfiteáter 1, 97401 Banská Bystrica, Slovakia*

*Faculty of Nuclear Science and Physics Engineering, Czech Technical University,
Břehová 7, 11519 Prague, Czech Republic*

Abstract

A Monte Carlo generator of the final state of hadrons emitted from an ultrarelativistic nuclear collision is introduced. An important feature of the generator is a possible fragmentation of the fireball and emission of the hadrons from fragments. Phase space distribution of the fragments is based on the blast wave model extended to azimuthally non-symmetric fireballs. Parameters of the model can be tuned and this allows to generate final states from various kinds of fireballs. A facultative output in the OSCAR1999A format allows for a comprehensive analysis of phase-space distributions and/or use as an input for an afterburner.

Key words: ultrarelativistic heavy-ion collisions, particle production, fragmentation, event-by-event fluctuations, correlations, Monte Carlo generator
PACS: 25.75.-q, 25.75.Dw, 25.75.Gz, 25.75.Ld, 25.75.Nq

Program summary

Program title: DRAGON

Catalogue identifier:

^{*} Supported in parts by VEGA 1/4012/07 (Slovakia), MSM 6840770039, and LC 07048 (Czech Republic).

Email address: boris.tomasik@umb.sk (Boris Tomášik).

Program summary URL: <http://www.fpv.umb.sk/~tomasik/dragon>

Program obtainable from: <http://www.fpv.umb.sk/~tomasik/dragon>

RAM required to execute with typical data: 100 Mbytes

Number of processors used: 1

Computer(s) for which the program has been designed: PC Pentium 4, though no particular tuning for this machine was performed.

Operating system(s) for which the program has been designed: Linux; the program has been successfully run on Gentoo Linux 2.6, RedHat Linux 9, Debian Linux 4.0, all with g++ compiler. It also ran successfully on MS Windows under Microsoft Visual C++ 2008 Express Edition as well as under cygwin/g++.

Programming language: C++

Size of the package: 32 818 bytes

Distribution format: tarred and gzipped archive

Number of lines in distributed program, including test data etc.: 6368

Number of bytes in distributed program, including test data etc.: 153 939

Nature of physical problem: Deconfined matter produced in ultrarelativistic nuclear collisions expands and cools down and eventually returns into the confined phase. If the expansion is fast, the fireball could fragment either due to spinodal decomposition or due to suddenly arising bulk viscous force. Particle abundances are reasonably well described with just a few parameters within the statistical approach. Momentum spectra integrated over many events can be interpreted as produced from an expanding and locally thermalised fireball. The present Monte Carlo model unifies these approaches: fireball decays into fragments of some characteristic size. The fragments recede from each other as given by the pre-existing expansion of the fireball. They subsequently emit stable and unstable hadrons with momenta generated according to thermal distribution. Resonances then decay and their daughters acquire momenta as dictated by decay kinematics.

Method of solving the problem: The Monte Carlo generator repeats a loop in which it generates individual events. First, sizes of fragments are generated. Then the fragments are placed within the decaying fireball and their velocities are determined from the one-to-one correspondence between the position and the expansion velocity in the blast wave model. Since hadrons may be emitted from fragments as well as from the remaining bulk fireball, first those from the bulk are generated according to the blast wave model. Then, hadron production from the fragments is treated. Each hadron is generated in the rest frame of the fragment and then boosted to the global frame. Finally, after all directly produced hadrons are generated, resonance decay channels are chosen and the momenta and positions of final state hadrons are determined.

Typical running time: Generation of 10^4 events can take anything between 2 hours to a couple of days. This depends mainly on the size and density of fragments. Simulations with small fragments may be very slow. At the beginning of a run there is a period of up to 1 hour in which the program calculates thermal weights due to statistical model. This period is long if many species are included in the simulation.

1 Introduction

In ultrarelativistic collisions of heavy atomic nuclei matter is probed at high temperature and density. The fireball thus created exists only for very short period of time; it quickly expands and hadrons decouple from it. If the collision energy is high enough, a phase of deconfined quarks and gluons is reached in the early phase of the collision. Due to pre-existing longitudinal movement of the incident nucleons and the inner pressure of the matter, it swiftly expands in longitudinal as well as transverse direction. At certain moment the energy density becomes too low to justify deconfinement and the matter hadronizes. From lattice QCD calculations we know that the change from deconfined to confined matter is rapid though smooth crossover in the region of the phase diagram at low baryochemical potential [1] and it becomes first order phase transition from certain value of μ_B upwards [2,3,4].

It is important for our discussion that the passage through this transition is very fast. In such a case, equilibrium description may be inapplicable and the phase transition would not proceed in the same way as probed on lattice. Instead, considerable supercooling can occur. In the region of the phase diagram where first order phase transition is expected even spinodal may be reached by the system if the expansion rate is bigger than the nucleation rate of bubbles of the new phase [5,6]. Then, the fireball disintegrates into droplets similarly to spinodal fragmentation known in liquid/gas nuclear phase transition [7].

Seemingly, such a mechanism should not work in the region of the phase diagram with smooth crossover. Nevertheless, it has been argued that an abrupt rise of bulk viscosity at T_c can suddenly make the fireball very stiff and if strong expansion is present in such a moment it can drive the system into fragmentation [8]. Hydrodynamic expansion in nuclear collisions is possibly unstable [9], thus fragmentation at hadronisation phase transition seems likely scenario.

On the other hand, hydrodynamically inspired parametrisations [10,11,12,13,14] combined with thermal models [15,16,17,18] provide satisfying description of single-particle spectra, particle abundances, and some also femtoscopy measurements. It is necessary to note that these are observables which are extracted from data *summed* over a large number of events. Event-by-event fluctuations of mean p_t [19,20,21] and angular correlations [22] indicate possible presence of clusters in momentum distributions. Such clusters could be due to fragmentation at the phase transition. Note that momentum clusters are buried under many entries to the histograms if summed over many events.

It is the purpose of the present Monte Carlo droplet generator to produce artificial data sets which resemble those coming from real nuclear collisions provided fragmentation occurs at hadronisation and hadrons are emitted from

fragments without any further scattering. Its name, DRAGON, stands for DRoplet and hAdron GeneratOr for Nuclear collisions. In a way, the model is similar to THERMINATOR [23], with the crucial difference that emission from fragments is included. Note that the code can write out the final state in OSCAR1999A format [24] and thus a possible further evolution of the hadronic cloud can be simulated with the help of a cascade generator.

In the next Section the model of particle emission from a fragmented fireball is reviewed. Section 3 explains the architecture of the program. Sections 4 and 5 explain how to install and run the generator. Some representative results are presented in Section 6 and the paper is concluded in Section 7. Details about generation of momenta from Boltzmann distribution are summarised in the Appendix.

2 The model of particle emission from fragmented fireball

In rapid phase changes the fireball can fragment and hadrons are emitted from the produced fragments. There may also be a portion of the produced hadrons which is emitted directly from the bulk fireball.

2.1 Hadrons produced from bulk

Directly produced hadrons are described by the *blast-wave model*. The Wigner distribution of their emission points and momenta is given as [13,25]

$$S(x, p) d^4x = \frac{2s + 1}{(2\pi)^3} m_t \cosh(y - \eta) \exp\left(-\frac{p^\mu u_\mu}{T_k}\right) \times \Theta(1 - \tilde{r}(r, \phi)) H(\eta) \delta(\tau - \tau_0) d\tau \tau d\eta r dr d\phi. \quad (1)$$

The model is formulated in terms of relativistic and polar coordinates r , ϕ , η , and τ

$$x^0 = \tau \cosh \eta \quad (2a)$$

$$x^1 = r \cos \phi \quad (2b)$$

$$x^2 = r \sin \phi \quad (2c)$$

$$x^3 = \tau \sinh \eta, \quad (2d)$$

while for momentum we use rapidity y , transverse mass (momentum) $m_t(p_t)$, and azimuthal angle ψ

$$p^0 = m_t \cosh y \quad (3a)$$

$$p^1 = p_t \cos \psi \quad (3b)$$

$$p^2 = p_t \sin \psi \quad (3c)$$

$$p^3 = m_t \sinh y. \quad (3d)$$

Emission points are distributed uniformly in radial direction for

$$\tilde{r} = \sqrt{\frac{(x^1)^2}{R_x^2} + \frac{(x^2)^2}{R_y^2}} < 1, \quad (4)$$

where

$$R_x = a R, \quad R_y = \frac{R}{a}, \quad (5)$$

with R being the mean transverse radius of the ellipsoidal fireball and a its spatial deformation parameter.

The distribution $H(\eta)$ specifies the profile of the fireball in space-time rapidity. Wigner density in eq.(1) is written in Boltzmann approximation and the factor $p_\mu u^\mu$ gives the energy of the produced hadron in the rest frame of the moving fluid. The fluid velocity field is parametrised as

$$u_\mu = (\cosh \eta \cosh \eta_t, \cos \phi_b \sinh \eta_t, \sin \phi_b \sinh \eta_t, \sinh \eta \cosh \eta_t), \quad (6)$$

$$\tan \phi_b = a^4 \tan \phi, \quad (7)$$

$$\eta_t = \tilde{r} \rho_0 \sqrt{2} (1 + \rho_2 \cos(2\phi_b)). \quad (8)$$

Finally, the factor $(2s + 1)$ in eq. (1) stands for the degeneration due to spin.

Formulated in this way, the fireball can have elliptic transverse shape controlled by the parameter a and elliptic transverse flow profile parameterized by ρ_2 .

2.2 Hadrons emitted by fragments

The fireball decays into fragments of spherical shape (in their rest frame). They are placed according to the distribution (1) with $T \rightarrow 0$, i.e. their velocity is identical the local fluid velocity at the place at which they were produced.

Fragments may come in one given volume b , if they are produced by mechanism which leads to one length scale which dominates the fragmentation—like spinodal fragmentation. Another possibility, implemented in the model is that the volumes are distributed according to gamma-distribution

$$\mathcal{P}_k(V) = \frac{1}{b\Gamma(k)} \left(\frac{V}{b}\right)^{k-1} \exp\left(-\frac{V}{b}\right), \quad (9)$$

with $k = 2$ [26]¹.

Fragments decay into hadrons exponentially in time, so the distribution of the emission time of a hadron in the rest frame of a fragment is

$$\mathcal{P}_t(\tau_d) = \frac{1}{R_d} \exp\left(-\frac{\tau_d}{R_d}\right) \quad (10)$$

where R_d is the radius of the droplet (fragment). Hadrons are produced from the whole volume of the fragment with uniform probability. Their momentum is chosen according to Boltzmann distribution with the temperature T_k in the rest frame of the fragment.

2.3 Resonance decays

Resonances may be produced from the fireball. Their lifetime is random according to exponential decay law $\exp(-\Gamma\tau)$ (in the rest frame of the resonance).

If a resonance with mass M decays via two-body decay to daughters with masses m_1 and m_2 , their energies will be

$$E_1 = \frac{M^2 - m_2^2 + m_1^2}{2M} \quad (11)$$

$$E_2 = \frac{M^2 - m_1^2 + m_2^2}{2M} \quad (12)$$

and they will be receding back-to-back (in the rest-frame of the resonance) with momenta

$$|\vec{p}_1| = |\vec{p}_2| = \frac{\sqrt{(M^2 - (m_1 + m_2)^2)(M^2 - (m_1 - m_2)^2)}}{2M}. \quad (13)$$

In case of three-body decays, in the rest-frame of the resonance, all the momenta of the daughter particles lay within a plane. Under the assumption of transition amplitude independent of momenta, the energy distributions of daughter particles are uniform. Thus there is some freedom in choosing the energies and momenta of daughter particles in such a way that the energy and momentum are conserved

¹ Note the different use of the parameter b here and in [26]: while there it has the dimension of inverse volume, here it has the dimension of volume. This brings it here on equal footing with the case when all fragments have the same volume.

$$E_1 + E_2 + E_3 = M \quad (14a)$$

$$|\vec{p}_1|^2 + |\vec{p}_2|^2 + 2|\vec{p}_1||\vec{p}_2|\cos\theta_{12} = p_3 \quad (14b)$$

where $E_i = \sqrt{|\vec{p}_i|^2 + m_i^2}$ and θ_{12} is the angle between the momenta \vec{p}_1 and \vec{p}_2 .

Daughter particles from a resonance decay may also be unstable. In that case, they will decay according to the same procedure.

2.4 Chemical composition

Relative abundances of the individual species follow the prescription of chemical equilibrium with temperature T_{ch} and chemical potentials for baryon number and strangeness μ_B , and μ_S . The density of species i is then given as

$$n_i(T_{ch}, \mu_b, \mu_S) = g_i \int \frac{d^3p}{(2\pi)^3} \left[\exp\left(\frac{\sqrt{p^2 + m_i^2} - (\mu_B B_i + \mu_S S_i)}{T_{ch}}\right) \mp 1 \right]^{-1} \\ = \frac{g_i}{2\pi^2} T_{ch}^3 I\left(\frac{m_i}{T_{ch}}, \frac{\mu_i}{T_{ch}}\right), \quad (15)$$

where the upper (lower) sign is for bosons (fermions), g_i is the degeneracy factor, and

$$I\left(\frac{m_i}{T_{ch}}, \frac{\mu_i}{T_{ch}}\right) = \int_0^\infty dx x^2 \left[\exp\left(\sqrt{x^2 + \frac{m_i^2}{T_{ch}^2}} - \frac{\mu_S S_i + \mu_B B_i}{T_{ch}}\right) \mp 1 \right]^{-1} \quad (16)$$

$$\mu_i = \mu_B B_i + \mu_S S_i. \quad (17)$$

From this, the probability that a random particle belongs to species i is

$$w_i(T_{ch}, \mu_B, \mu_S) = \frac{n_i(T_{ch}, \mu_B, \mu_S)}{\sum_i n_i(T_{ch}, \mu_B, \mu_S)}, \quad (18)$$

where the sum in the denominator runs through all the species.

3 Programming structure and solution

The structure of the program is outlined in Figure 1. It is written in C++. The code is split into three files: `dropem.cpp` includes the main function and functions for reading and initialising resonance decays and for their decay. The file `dgener.cpp` defines classes needed for the working of the MC generator, and `specrel.cpp` defines basic vectors and tensors and operations with them.

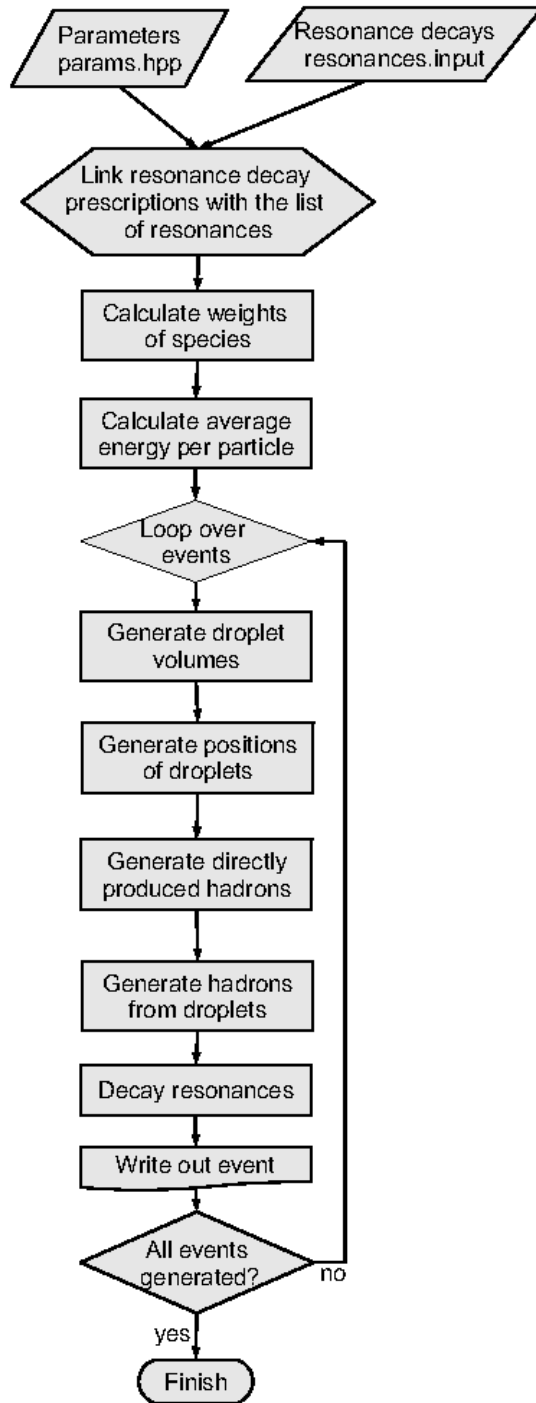


Fig. 1. The structure of the program.

3.1 *Introductory phase*

Parameters of the model and steering constants for compiling and running are specified in the file `params.hpp`. This also includes the list of all species

called `pproperties`. This is an array, whose entries are records for individual species. In the current version we standardly include all baryons with masses up to $2.0 \text{ GeV}/c^2$ and mesons up to $1.5 \text{ GeV}/c^2$.

Resonance decays are listed in a separate input file `resonances.input`. A file with this name must be present in the directory in which the program is running. It lists the modes in which resonances can decay. If at least one decay mode for given species is listed in this file, that species is treated as an unstable resonance and, vice versa, if species is not listed in the resonance file, it is stable. In order to store data of all decay modes of a resonance and simulate the decay of resonances, a class `DecayPattern` is defined in file `dgener.cpp`. After all decay prescriptions are read in, a link to the corresponding `DecayPattern` is added to each record of unstable species in `pproperties`. Vice versa, daughter particle species defined in the decay modes are linked to their properties in `pproperties`.

Subsequently, weights for generation of all species are calculated according to eq. (18) and stored for each sort of hadrons in the list `pproperties`.

At the end of the initial phase, average energy of hadron at the specified chemical composition and kinetic temperature is determined. This allows to translate the expected multiplicity (specified as input parameter) into the energy which is contained in the fireball or the fragments. With the help of the energy density this is translated into the expected volume of the fragments. This later controls the number of generated fragments.

3.2 Loop over events

The number of events to be generated is given as a macro `NOEvents` in parameter file `params.hpp`. The loop is repeated this number of times.

DRAGON can generate fireballs with ellipsoidal cross-section, so first the direction of the event plane is chosen randomly. Thus each event has a different reaction plane as it is the case in real data.

In the next step, sizes of fragments are either generated according to gamma-distribution, eq. (9), or they are set all to the same value. Their number is chosen so that the energy which they contain corresponds to the multiplicity to be produced from fragments.

The sizes, if they are not all equal, are then sorted with the help of a quick-sort algorithm. This is done in order to facilitate placing of the fragments in the reaction volume. Their positions are generated randomly as specified in Section 2.2. Rapidity of the fragments is chosen randomly according to either

Gaussian distribution with specified mean and width, or uniform distribution between specified minimum and maximum. Transverse position is chosen uniformly within the ellipsis with radii R_x and R_y . The direction of R_x is parallel to the event plane. Velocity of the fragment is then specified by eq. (6). For each fragment, after its position is generated, it is checked if it does not overlap with any of the previously allocated fragments. If so, the position is generated anew. The algorithm starts with large fragments and continues to the smaller ones; otherwise there could appear problems with placing the big fragments at the end.

Once all fragments are placed within the fireball, hadrons emitted from the bulk (not from fragments) are generated. This begins with determining the type of hadron according to the probabilities calculated in the initial stage. After this, the thermal component of hadron momentum is generated according to Boltzmann distribution with temperature T_k . Rejection method is used; more details can be found in the Appendix. The direction of the momentum is random with isotropic distribution. The position from which hadron is emitted is chosen according to the emission function in eq. (1) with the same rapidity distribution as was used for fragments. The position corresponds to some value of the collective expansion velocity via eq. (6). The generated momentum is then boosted by this velocity. It is also checked that the generated particle is not produced within some of the fragments. If so, its position is rejected and generated again. The whole procedure is repeated until the expected number of hadrons from the bulk is generated.

Hadrons emitted from fragments are generated in a similar way as those from the bulk. In the rest frame of the fragment, energy and momentum are generated according to Boltzmann distribution and the position according to homogeneous distribution. The times of emission are distributed exponentially, as seen from eq. (10). Finally, hadron position and momentum are boosted by the velocity of the fragment and the position is also shifted by the initial position of the fragment. After the generation of each hadron it is checked whether the energy contained in all hadrons from given fragment so far does not exceed the total energy of the fragment. If it does, no more hadrons are generated from that fragment. Thus energy and momentum are not strictly conserved in hadron emission from fragments. This is not bothering as long as the energy and momentum of the fragment are unknown in the experiment.

The next step is to decay resonances. This is performed by void function `DecayResonances`. All hadrons are stored in a First-In-First-Out stack of particle records. The record for each particle includes a link to its decay prescription; if the particle is stable then no link is present. The stack also keeps the number of particles. The algorithm counts stable particles. It takes one particle from the stack. If it is stable, the particle is put back into the stack and the counter of stable particles is increased by one. If it is unstable, then

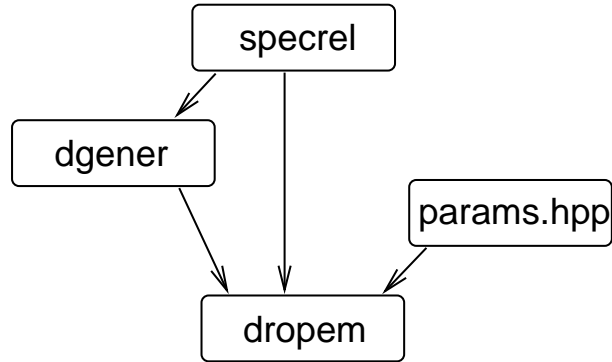


Fig. 2. Dependences of the source files.

decay is initiated. The counter of stable particles is reset to 0 and daughter particles are put into the stack. This is repeated until the counter of stable particles reaches the number of particles in the stack.

To simulate the decay of a resonance the algorithm first chooses the decay channel according to branching ratios. Momenta of daughter particles in the rest frame of the fragment are determined as explained in Section 2.3. These momenta are first rotated so that their orientation is distributed isotropically and then boosted by the resonance velocity. Then, a time in which the resonance decays is generated according to the exponential decay law. The position in which the resonance finds itself at that time is the initial position of the daughter particles.

When all resonances are decayed, generated hadrons are written into the output file.

4 Installing DRAGON

The droplet generator DRAGON is distributed as a package with three C++ header files (`specrel.hpp`, `dgener.hpp`, `params.hpp`), three C++ source files (`specrel.cpp`, `dgener.cpp`, `dropem.cpp`), an input file with resonance decays (`resonances.input`) and Makefile for easy compiling on Linux.

The dependences of individual source files in the distribution package are illustrated in Figure 2. Their content is as follows:

specrel contains prototypes (`.hpp`) and definitions (`.cpp`) of objects for four-vectors and three-vectors together with operations on them, like addition and multiplication with Minkowski metric, where applicable. Also tensors and their operations are introduced. There are functions for boosting four-vectors to other reference frames. Also an object `Particle` is defined which stores properties, momentum and emission position of a particle.

dgener (.hpp and .cpp file) introduces specific technical tools which are used in the random generator.

dropem.cpp contains the main routine with the code according to algorithm outlined in Section 3.

params.hpp is the header file with settings and values for parameters which are used in the generation. This file can be edited in order to compile and run the generator with a different set of parameters.

resonances.input is input data file which should be present (under this name) in the directory in which the generator is running.

The generator should compile and run on any system with standard C++ compiler. It has been tested with **g++** on Gentoo Linux 2.6, RedHat Linux 9, Debian Linux 4.0. It also ran successfully on MS Windows under Microsoft Visual C++ 2008 Express Edition as well as under cygwin/g++.

5 Running DRAGON

On Linux, **Makefile** makes sure that executing the **make** command will compile, link and prepare the executable file **dragon.exe** correctly. If **make** cannot be used, then one should follow the commands as they appear in the **Makefile**. Visual C++ by Microsoft will compile and link the code if all .cpp and .hpp files are included.

The executable **dragon.exe** is run with one or two parameters like e.g.

```
> dragon.exe outfile.out dropinfo.out
```

The first parameter is the name of the output file, where generated particles will be written out by the program, in an output format which can be chosen. The second parameter, which is optional, stores information about the droplets which have been generated in each event. If the second parameter is not given, this information is not written out. If parameters are omitted, then the default output file **DRAGON_events.out** is chosen. A file **resonances.input** must be present in the directory where the program is being run.

5.1 Input

Settings for the program and parameters are chosen before the compilation in the file **params.hpp**. They are also explained in the comments within the file. Here, they are explained in more detail:

NOEvents is the number of events which shall be generated

RANDOMDROPLETS is a logical constant; which is set either to 1, if the volumes of fragments are to be set randomly according to eq. (9), or to 0 if all fragment volumes should be equal

OVERLAPFORBIDDEN is by default set to 1; it can be set to 0 if the user wants to allow an overlap of fragments. The latter choice is unrealistic, but may be useful in some special studies, since forbidding fragment overlap leads to some anticorrelation of momenta when hadrons from different droplets are usually unlikely to have similar momenta.

GAUSSIAN_RAPIDITY is a logical constant which is set to 1 if the rapidity profile of the fireball should be Gaussian and to 0 for uniform rapidity profile

ACCEPTANCECUT declares which hadrons should be written out to the output file. This can be used to formulate simple conditions for detector acceptance. The macro which is defined here is a logical statement which is evaluated for each particle before it is written out. Following kinematic variables can be used: rapidity (defined as variable `yrap`), transverse momentum (`pT`), or azimuthal angle (`Phi`). The condition can be, e.g.

```
#define ACCEPTANCECUT ((yrap>-1.)&&(yrap<=1.))
```

i.e. hadrons with rapidity between -1 and 1 are recorded.

WRITEOUT is an optional string which is written in the header part of the output file if it is in OSCAR1999A format [24]. By default, it is left empty. If a newline command ‘\n’ appears, it should be followed by ‘#’, which starts a comment line in OSCAR1999A format.

short FORMAT is an identifier of the format of the output file. Currently, four possible output formats are predefined. They are explained in the comments. Note that in the OSCAR1999A format two numbers in each line are added to the standard output. The last number is 1 if the hadron described in that line comes from resonance decay and 0 otherwise. The next to last number identifies the fragment from which the hadron (or its parent resonance) stems; and is -1 for hadrons not originating from any fragment.

BIGMASS is set to 10. by default. This is the parameter B described in the Appendix below equation (A.3). Its setting requires some fine-tuning and we do not recommend to change it.

Anr is set to 20. by default. This is the parameter A described in the Appendix in eq. (A.6). It is not recommended to change it.

double fotemp is the *kinetic* freeze-out temperature in units of GeV.

double Tch is the *chemical* freeze-out temperature in units of GeV.

double mub is the baryochemical potential in GeV.

double mus is the chemical potential for strangeness in GeV.

double huen is the energy density within the fragments, in units of $\text{GeV}\cdot\text{fm}^{-3}$.

double minrap is the minimum rapidity of fragments or directly produced hadrons which will be generated.

double maxrap is the maximum rapidity of fragments or directly produced hadron which will be generated, so fragments and direct hadrons are generated with rapidities between `minrap` and `maxrap`.

double dNdy_total is the dN/dy of *all* hadrons which roughly should be generated. This variable is useful in case of uniform rapidity distribution and is only used for calculation of **N_total** (see next). If it is not used there, it can be commented out.

double N_total is the total expected multiplicity in the interval between rapidities **minrap** and **maxrap**. For a uniform rapidity distribution it can be conveniently calculated as

```
double N_total = dNdy_total * (maxrap-minrap);
```

It can also be set equal to a given number.

double DropletPart is a parameter between 0 and 1 which determines the fraction of all hadrons that stem from the decay of fragments. It is 1 if all hadrons are produced from fragments and 0 if they all are emitted directly from the bulk fireball.

double rapcenter is only relevant for Gaussian rapidity distribution and gives the rapidity of the centre of the rapidity profile. It is irrelevant if uniform rapidity distribution is chosen.

double rapwidth is the width of Gaussian rapidity distribution and is irrelevant if uniform rapidity distribution is chosen.

double rb is the radius, in fermi, of the fireball which decays into fragments and/or hadrons. It appears as R in eq. (5).

double a_space is the spatial anisotropy parameter a as it appears in eq. (5).

double tau is the parameter τ_0 from eq. (1), in units of fm/ c .

double etaf is the parameter ρ_0 from eq. (8).

double rho2 is the parameter ρ_2 from eq. (8).

double b is the parameter b of the gamma-distribution of fragment sizes in eq. (9), if **RANDOMDROPLETS** is set to 1. In case that **RANDOMDROPLETS** is set to 0, this gives the volume of fragments.

long int seed is the initial seed for pseudo-random generator. If this is set to 0, the generator is initiated with machine time.

int NOSpec is the number of species which can be generated in the simulation.

PChem pproperties [] is a vector of structures **PChem** which store the records of properties of individual species. The vector has as many entries as specified by **NOSpec**. For one species, these properties must be given (in this ordering),

- (1) Monte Carlo ID number of species according to Particle Data Group [27]; integer
- (2) mass in GeV/ c^2 ; double
- (3) baryon number; integer
- (4) strangeness; integer
- (5) 1 if the species is boson or 0 if it is fermion
- (6) spin degeneracy; integer
- (7) put 1. here, double; (this will be calculated later by the program)
- (8) put another 1. here, double; (this will be calculated later by the pro-

```

# rho+
213      0.766   0.150
1.       211     0.13957  111  0.13498

# rho0
113      0.769   0.151
1.       211     0.13957  -211 0.13957

# rho-
-213     -1.     0.150
1.       -211    -1.     111  -1.

# omega
223      0.782   0.00844
0.888    -211    0.13957  111  0.13498  211  0.13957
0.0221   -211    0.13957  211  0.13957
0.085    111     0.13457  22  0.

# eta' (958)
331      0.95778 0.000203
0.445    211     0.13957  -211 0.13957  221  0.54751
0.294    113     0.769    22  0.
0.208    111     0.13498  111  0.13498  221  0.54751
0.0303   223     0.782    22  0.
0.0212   22      0.       22  0.

```

Fig. 3. An excerpt from the file `resonances.input`.

- gram)
- (9) put `-1` in the last position, integer; this will be also determined by the program and will link the species to its decay prescriptions; it will remain `-1` for stable particles.

Data entries for one species are divided by commas. Record for one species should be input within curly brackets.

Decays of resonances are listed in the file `resonances.input`. The structure of the records in that file is as follows (an example of the file `resonances.input` is shown in Figure 3):

- A record of all decay modes of one resonance starts with a line with three numbers: MC code (identifier) of the resonance, its mass in GeV, and its width in GeV. If `-1` is put in the position of the mass, the code automatically reads in the mass from `pproperties []`.
- Record of a two-body decay contains five numbers. First, there is branching ratio for the decay channel, which must be multiplied by the Clebsch-Gordan coefficient, if applicable. This is followed by MC code of the first daughter particle and its mass, and the same for the second daughter particle. Again, if `-1` is put instead of the mass, the mass it fed in automatically.
- Three-body decays are recorded with seven numbers, where MC code of the third daughter particle and its mass are added to the structure of the record of two-body decays.

If the sum of branching ratios is not unity, the program will multiply them with a common factor so that their sum will become 1. Decays into photons (or leptons) can also be included with the appropriate MC codes (e.g. 22 for photons). Any line that starts with “#” or is empty is considered as a comment. Comments are very useful in order to enhance the readability of the records.

5.2 Output

Output data are directed into the file which is specified as a command line parameter. The possible formats for the output are explained as comments in `params.hpp`. Note that in case of the OSCAR1999A output format each line contains also two additional output numbers: On the 13th position the number of the fragment from which the hadron originates, or the number from which its parent resonance was emitted. For hadrons emitted from bulk this number is -1 . On 14th position there is 0 if this is directly produced hadron or 1 if the hadrons stems from a resonance decay.

If droplet information is stored, the file will contain lines with the following structure: event number, number of droplet, rapidity of droplet, transverse velocity of droplet, azimuthal angle of its transverse velocity. This is followed by the multiplicities of individual sorts of particles which are emitted from the given droplet. Thus for example a record like

```
# eid d_id rapidity v_t phi sorts:
#                               -211 111 211
...
# 2   3   1.2724   0.3411   2.4513   12   10  16
```

means that in event 2 we have droplet number 3, which moved with rapidity 1.2724 and transverse velocity $0.3411c$ under azimuthal angle 2.4513 rad. From this droplet 12 π^- s (code -211), 10 π^0 s (code 111), and 16 π^+ s (code 211) are emitted. (Usually, one would make simulation with many more species; we only show three here for brevity.)

6 Sample results

6.1 Size of droplets

In order to get an impression of the size of droplets, we first give average numbers of final state hadrons coming from one droplet for various settings of

parameters. Resonances were included in this calculation. They decayed into stable hadrons and here the final numbers of stable hadrons are given. They were all calculated for energy density and chemical freeze-out conditions at RHIC $T_{ch} = 168$ MeV, $\mu_B = 266$ MeV, $\mu_S = 71$ MeV. For small droplets with the volume of 2 fm^3 and kinetic temperature 160 MeV, there are on average 2.3 pions, 0.2 nucleons, and 3.2 hadrons in total produced. For the volume 10 fm^3 the corresponding numbers are 8.7, 0.9, and 12.1. For very large volume like 100 fm^3 we have on average 80.9 pions, 7.8 nucleons, and 112.3 hadrons. The temperature dependence is rather weak, e.g. in the latter case dropping the temperature from 160 to 100 MeV increases the pion number to 94. In general, lower kinetic temperature leads to larger number of hadrons since less energy is used in the form of kinetic energy.

6.2 Comparison with THERMINATOR

DRAGON is similar to THERMINATOR [23], with some differences:

- DRAGON allows for particle emission from fragments; in fact this was the main motivation for conceiving it.
- The radial profile of transverse expansion velocity grows linearly in DRAGON (cf. eq. (8)), while it is kept at constant value if the blast wave model option is set in THERMINATOR.
- THERMINATOR also simulates freeze-out in Cracow single freeze-out model [14] and in blast wave model with varying time dependences of radial coordinate of the freeze-out hypersurface [28].
- DRAGON allows to simulate azimuthally non-symmetric fireballs.
- THERMINATOR uses SHARE [15,29] to define chemical composition and resonance decays. The list of included resonances and decays is longer than that of DRAGON, which should not cause a problem, however, as higher lying states are suppressed by Boltzmannian factor.

The results of both models are compared in Figure 4. For this comparison, THERMINATOR was run with the set of parameters with which it is distributed, just the freeze-out model was set to be blast wave and not the Cracow single freeze-out. Parameters of DRAGON were chosen correspondingly. Note that multiplicity results from the chosen parameters in THERMINATOR while it is set by hand in DRAGON. Thus the difference in absolute normalisation of the spectra is irrelevant. Recall, that the transverse flow expansion rapidity 0.55 was constant irrespective of radial coordinate in THERMINATOR; in DRAGON we chose $\rho_0 = 0.55$. This leads to the same mean transverse expansion velocity.

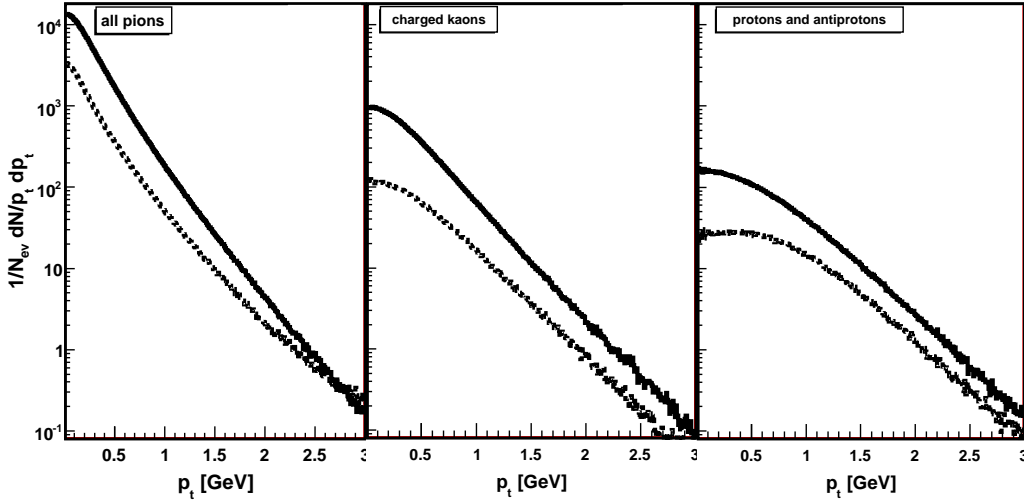


Fig. 4. Comparison of p_t spectra generated by DRAGON (solid lines) and THERMINATOR [23] (dotted lines). In THERMINATOR the blast-wave source was chosen with the parameters that come with the standard distribution: $v_r = 0.55$, $\tau = 9.74$ fm/ c , $\rho_{\max} = 7.74$ fm, $T = 165.6$ MeV, $\mu_B = 28.5$ MeV, $\mu_S = 6.9$ MeV. Parameters were chosen correspondingly in DRAGON with $\rho_0 = 0.55$. Spectra from 10^4 simulated events are shown.

In Figure 4 we observe this difference. At low p_t , THERMINATOR spectra are suppressed against DRAGON. These are the hadrons with low transverse velocities. In DRAGON, they are produced mainly from regions of the fireball which move slowly outwards. In THERMINATOR, such regions are missing (since transverse velocity is everywhere the same) and this leads to the effect on the spectra. Pions move relativistically already at rather low p_t , so for them this suppression is at *very* low p_t and is almost invisible. On the other hand, at very high transverse momentum their spectra become flatter in THERMINATOR. These are pions which move with *very high* transverse velocities—higher than the transverse expansion velocity of the fireball. In THERMINATOR, their production is enhanced by the fact that we have larger region that moves outwards with rather large transverse velocity. In other kinematic regions—high p_t for kaons and protons and semi-low p_t for pions—the spectra from DRAGON and THERMINATOR are parallel and consistent.

6.3 Single-particle spectra

Results obtained from a simulation with Gaussian rapidity profile, are illustrated in Figures 5, 6, and 7. First of them shows the rapidity spectra. In the simulation, space-time rapidity distribution was centered at $\eta = 0$ with a width of 1.3 and kinetic freeze-out temperature $T_k = 160$ MeV. We show

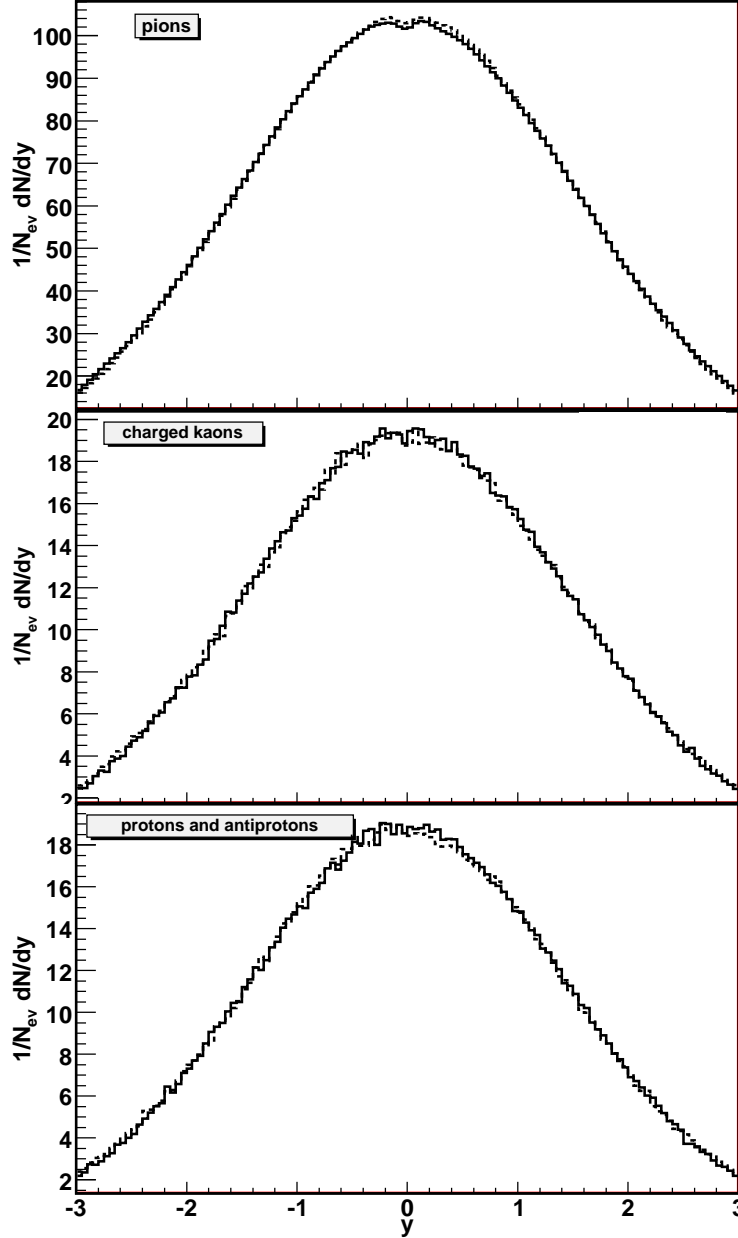


Fig. 5. Comparison of rapidity spectra from a model with fragments (solid lines, $b = 50 \text{ fm}^3$) and without them (dotted lines) for charged pions (top), kaons (middle), and protons and antiprotons (bottom). A model with Gaussian space-time profile was chosen with the width $\Delta\eta = 1.3$. Other parameters were: $T_k = 160 \text{ MeV}$, $T_{ch} = 168 \text{ MeV}$, $\mu_B = 266 \text{ MeV}$, $\mu_S = 71 \text{ MeV}$, $\rho_0 = 0.6$. Spectra from 10^4 simulated events are shown.

results from simulations with and without fragments. Note, that in case of fragments their typical size is actually chosen rather large ($b = 50 \text{ fm}^3$). No difference is observed between the spectra obtained from the two kinds of simulation. This is expected: fragmentation of the fireball cannot be seen from observables integrated over large number of events.

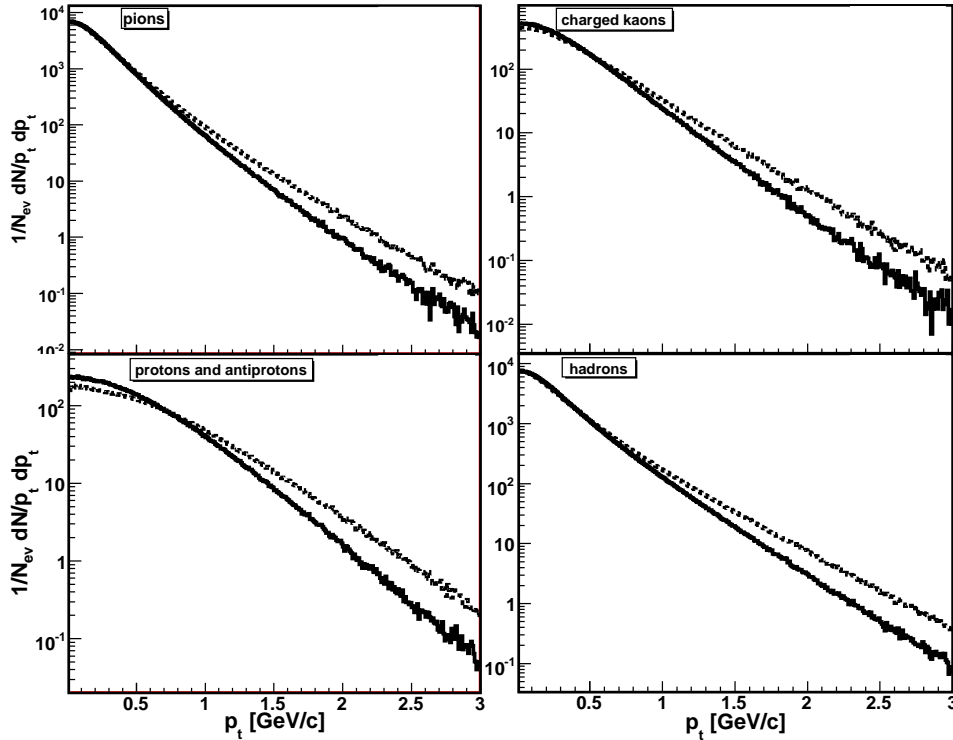


Fig. 6. The p_t spectra from a model with Gaussian space-time rapidity profile with the width $\Delta\eta = 1.3$. Results from the same simulation as in Fig. 5: $T_k = 160$ MeV, $T_{ch} = 168$ MeV, $\mu_B = 266$ MeV, $\mu_S = 71$ MeV, $\rho_0 = 0.6$. Spectra from 10^4 simulated events are shown; they are integrated over rapidity. Solid lines show results from a simulation with fragments with $b = 50 \text{ fm}^3$ and dotted lines show results from a simulation without fragments.

The same conclusion can be drawn from the p_t spectra. The spectra from non-fragmented fireball appear slightly flatter. This is because in such a simulation particles can be produced from regions close to the radial edge of the fireball which move with highest transverse velocity. Fragments are produced in such a way that their volume is always completely included in the volume of the fireball and their velocity corresponds to the fireball expansion velocity at the *centre* of the fragment. Thus fragments (especially the big ones) can never obtain as high transverse velocity as the hadrons in non-fragmented fireball. In a case where both simulations are performed with the same ρ_0 , like in Fig. 6, simulation without fragmentation thus yields slightly flatter p_t spectra.

In Fig. 7 we show the contributions to pion spectra. In both cases, with and without the fragments, they are the same. The most important contribution at this chemical freeze-out temperature ($T_{ch} = 168$ MeV, $\mu_B = 266$ MeV, $\mu_S = 71$ MeV) comes from resonance decays. Direct pion production becomes equally important at around $p_t = 1.5$ GeV/c.

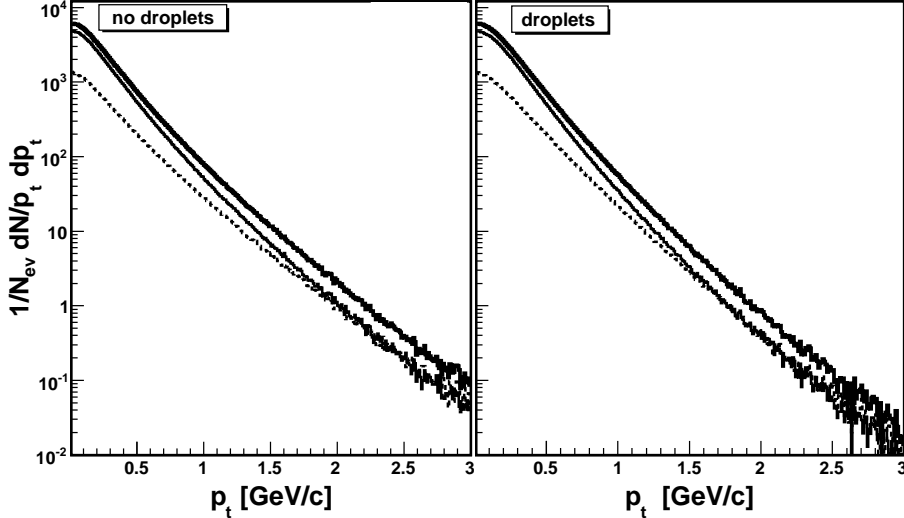


Fig. 7. The contributions to pion spectra from the simulations of Fig. 6. Thin solid line is the resonance contribution, dotted line shows direct pion production and thick solid line is the total resulting spectrum. Left: simulation without fragments (droplets), right: simulation with fragments (droplets) with $b = 50 \text{ fm}^3$.

6.4 An illustration of fragments

As mentioned, fragmentation cannot be observed in spectra integrated over a large number of events. Correlation and fluctuation observables go beyond the scope of this paper and shall be investigated in subsequent dedicated papers. Just to illustrate the production from fragments, momenta and positions of particles are illustrated in Figure 8. Positions of emission points (right column) and momenta of hadrons (left column) in rapidity and azimuthal angle are shown. In this illustration only directly emitted pions have been considered for the sake of simplicity. In the top row we show momenta and positions of the emission for a fireball that expands boost invariantly in longitudinal direction. It is observed that both positions and momenta spread uniformly over the whole (η, ϕ) interval. In order to clearly illustrate the effect of fragments on the momentum distribution, in the bottom row results from an event with large fragment volume ($b = 50 \text{ fm}^3$) and very low kinetic freeze-out temperature ($T_k = 10 \text{ MeV}$) are shown. The large volume ensures that there are many pions coming from one fragment and the low temperature puts a limit on their thermal velocity so that it stays close to that of the fragment. Thus clustering of the emission points is transferred to the momentum space. Note, however, that the values of parameters are unrealistic. In order to show results in a more realistic simulation, in the middle row a temperature $T_k = 170 \text{ MeV}$ was chosen. The clustering in momentum space is still observed though now it is much less pronounced. Note that in realistic situation (i) the size of fragments will probably be smaller; (ii) the number of fragments will be bigger; (iii) also other hadron species shall be present and pions shall dominantly be produced

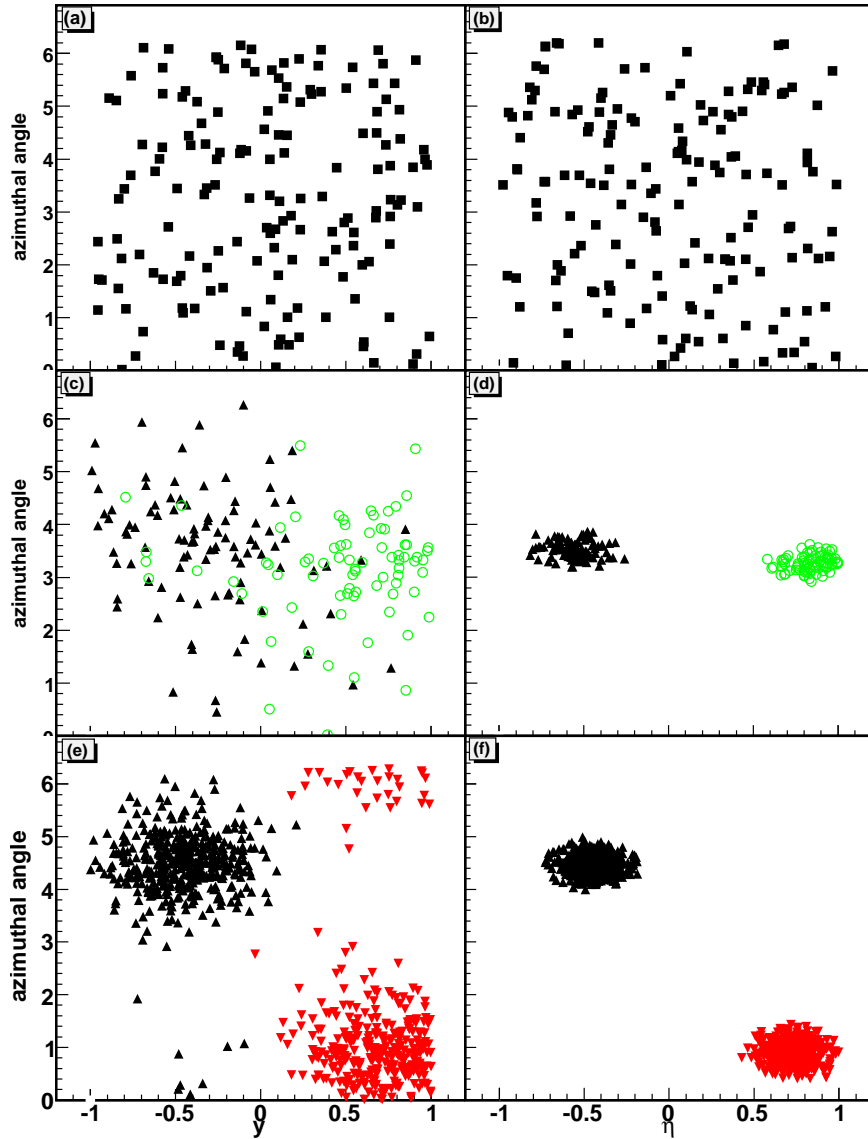


Fig. 8. Positions in space-time rapidity η and azimuthal angle from which pions were emitted (right column) as well as rapidities and azimuthal angles of the momenta which they had (left column). No resonances and no other particles than pions were produced here. Top row: pions emitted from boost-invariantly expanding fireball which does not fragment. Middle row: pions emitted from two large fragments with temperature 170 MeV. Hadrons from the same fragment are indicated by the same symbol. Rapidities, transverse velocities, and azimuthal angles of the fragments are $(-0.55, 0.51c, 3.53 \text{ rad})$ and $(0.84, 0.47c, 3.30 \text{ rad})$ and they emit 139 and 123 pions. Bottom row: as middle row but for the sake of illustration the temperature was set to 10 MeV. Rapidities, transverse velocities and azimuthal angles of the two fragments are $(-0.44, 0.45c, 4.49 \text{ rad})$ and $(0.73, 0.34c, 0.92 \text{ rad})$ and they emit 435 and 390 pions.

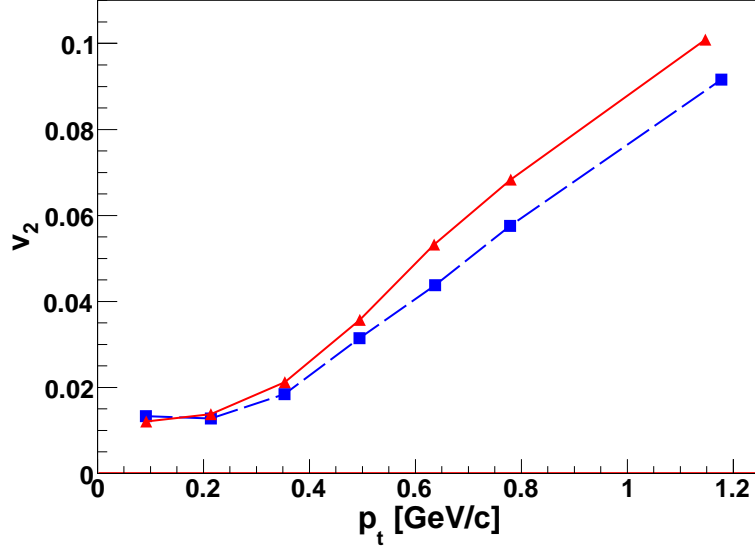


Fig. 9. The elliptic flow parameter v_2 of all hadrons calculated for parameters of the blast wave model that have been fitted to Au+Au collisions at $\sqrt{s} = 130$ AGeV, centrality class for elliptic flow 11–45% [30]: $T_k = 107$ MeV, $\rho_0 = 0.85/\sqrt{2}$, $\rho_2 = 0.058$, $R = 11.1$ fm, $a = 0.939$, $\tau = 7.7$ fm/c [13] and $T_{ch} = 174$ MeV, $\mu_B = 46$ MeV, $\mu_S = 13.6$ MeV [17]. Solid red lines with triangles show results from simulation with fragments ($b = 10$ fm³) and dashed blue lines with squares show results from simulation where all hadrons have been produced from the bulk fireball.

from resonance decays. Thus clustering in momentum space shall be even less visible and sophisticated methods might be necessary in order to identify fragmentation.

6.5 Elliptic flow

An important observable is the elliptic flow. This model provides the possibility to simulate azimuthally non-symmetric collisions where elliptic flow is observed. Within the blast wave model, the existence of azimuthal anisotropy of single particle spectra can be achieved by setting the spatial anisotropy a and/or the expansion velocity anisotropy ρ_2 [25]. In order to illustrate the elliptic flow, we calculated v_2 for a set of parameters which reproduce mid-central Au+Au collisions at $\sqrt{s} = 130$ AGeV [13] (Figure 9).

The elliptic flow parameter v_2 was determined from simulated data via two-particle correlations in the azimuthal angle

$$v_2(p_t) = \left[\frac{\int d\Delta \cos(2\Delta) N_2(\Delta, p_t)}{\int d\Delta N_2(\Delta, p_t)} \right]^{1/2} \quad (19)$$

$$N_2(\Delta, p_t) = \frac{1}{2} \int d\phi_1 \int d\phi_2 \delta(\Delta - |\phi_1 - \phi_2|) N_1(\phi_1, p_t) N_1(\phi_2, p_t), \quad (20)$$

where $N_1(\phi, p_t)$ is the single-particle distribution in azimuthal angle and transverse momentum. In practice, v_2 is not evaluated for a sharp value of the transverse momentum, but momenta from an interval in p_t are taken. In this analysis, the p_t range was divided into seven intervals.

In Fig. 9 we compare the elliptic flow for all hadrons calculated in a standard blast wave model with one calculated in case of all hadrons emitted from fragments. In both cases, all parameters of the model were the same; only the percentage of particles coming from fragments is 0 in one and 100% in the other case. A slight increase of the elliptic flow in case of fragmented fireball is observed. This is due to enhanced correlations of hadrons from one fragment. A thorough investigation of the elliptic flow from fragmented fireball shall be deferred to a dedicated paper.

7 Conclusions

The new Monte Carlo generator of the final positions and momenta of hadrons represents the blast wave model and incorporates important additional features. Above all it is the possibility to simulate hadron emission from a fragmented fireball. It is possible to vary the planned multiplicity and the percentage of particles which are emitted from the fragments. Additionally, it also allows for simulation of azimuthally non-symmetric events. THERMINATOR, the closest related model on the market, exists only in the azimuthally symmetric version.

Thus two kinds of studies can be envisaged for which DRAGON appears unique: (i) studies of correlations and fluctuations connected with fragmentation of the fireball; (ii) studies of spectra and correlations in non-central collisions. The main driving motivation for its development was the former, as fragmentation may be intimately connected with the dynamics of the phase transition. The Monte Carlo generator can be used for designing and testing new observables for probing fragmentation.

Acknowledgment I appreciate discussions with Marcus Bleicher, Andrew Jackson, Igor Mishustin, Ivan Melo, and Giorgio Torrieri. I thank Giorgio Torrieri for running the THERMINATOR model and for discussions which helped to debug the code. I also thank Michal Vagač for the computer support.

A Momentum generation from Boltzmann distribution

In this appendix it is reviewed how the momenta of hadrons are generated according to Boltzmann distribution, in the rest-frame of the fragment or fluid element.

First, the case $T_k = 0$ is treated separately. In such a case the momentum vanishes and the energy is put equal to the hadron mass.

For non-zero temperatures, *rejection method* is used to generate the size of the momentum. The Boltzmann distribution is

$$\mathcal{P}_B(p) \propto p^2 \exp\left(-\frac{\sqrt{m^2 + p^2}}{T}\right). \quad (\text{A.1})$$

If the mass of the hadron is small with respect to T , this distribution receives large contribution from the region of high momenta. Momentum is first generated according to gamma distribution

$$\Gamma_3(p) \propto p^2 \exp\left(-\frac{p}{T}\right), \quad (\text{A.2})$$

which is implemented as explained in [31]. Once momentum p is generated, it is accepted with probability

$$\mathcal{P}_{\text{acc}} = \exp\left(\frac{p - \sqrt{m^2 + p^2}}{T}\right). \quad (\text{A.3})$$

The natural scale for the mass is the temperature. In the code, this procedure is used for masses smaller than $B \cdot T$, where the parameter B is introduced as macro `BIGMASS` and is normally put equal to 10. Acceptation probabilities of some light particles are shown in Figure A.1.

For large masses, this procedure becomes ineffective because the acceptance probability is tiny if $p \ll m$. In this case, the problem can be treated non-relativistically. All three components of the momentum are generated according to the non-relativistic distribution

$$\mathcal{P}_{\text{nr},i}(p_i) \propto \exp\left(-\frac{p_i^2}{2mT}\right). \quad (\text{A.4})$$

Thus total momentum will satisfy the distribution

$$\mathcal{P}_{\text{nr}}(p) \propto p^2 \exp\left(-\frac{p^2}{2mT}\right). \quad (\text{A.5})$$

This cannot be used in the rejection method in a strict way, because distribution (A.5) drops for large p as $e^{-\alpha p^2}$ whereas the correct relativistic distribution

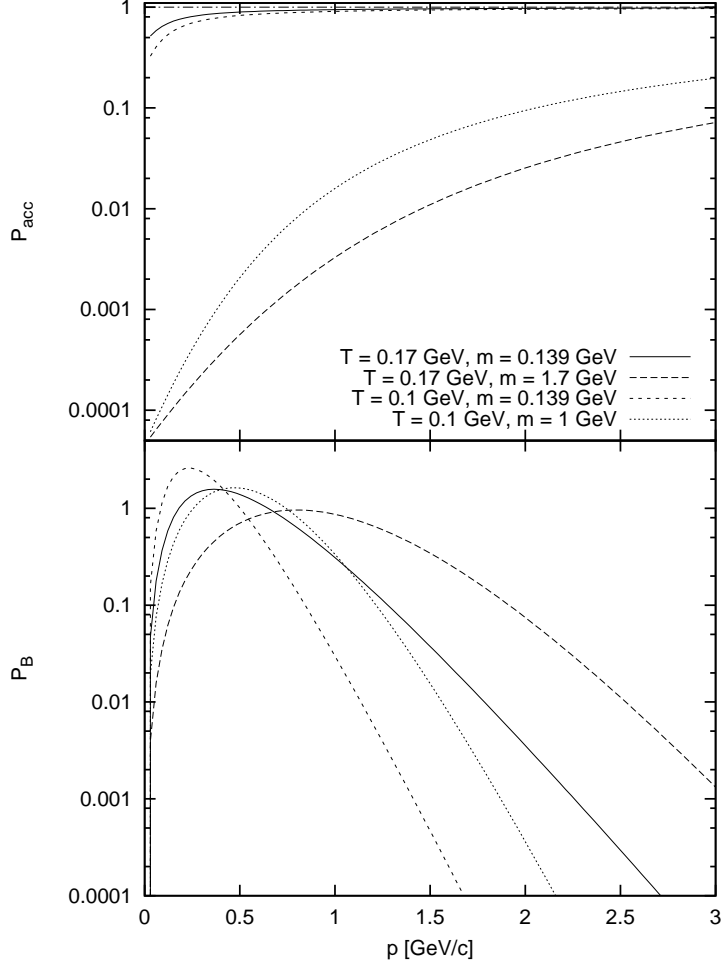


Fig. A.1. Top: The acceptance probability for light hadrons for some combinations of mass and temperature calculated from eq. (A.3). Bottom: Boltzmann distribution of momenta for light hadrons.

(A.1) goes like $e^{-\beta p}$. Thus there will always be a region of large p in which $\kappa\mathcal{P}_{\text{nr}}(p)$ becomes smaller than $\mathcal{P}_B(p)$ no matter the value of the multiplier κ . The acceptance probability calculated as $\mathcal{P}_B(p)/\kappa\mathcal{P}_{\text{nr}}(p)$ then becomes bigger than 1.

In the implementation, the constant κ is chosen in such a way that the acceptance probability becomes 1 at $p = AT$. Thus the acceptance probability then is

$$\mathcal{P}_{\text{acc}} = \exp\left(\frac{p^2}{2mT} - \frac{\sqrt{m^2 + p^2}}{T}\right) \exp\left(-\frac{A^2T}{2m} + \sqrt{\frac{m^2}{T^2} + A^2}\right). \quad (\text{A.6})$$

This technically means that for p larger than AT all hadrons with momenta generated according to non-relativistic distribution are accepted. It also means that in the spectrum these are suppressed relative to the case where they would be generated according to the correct distribution, due to faster decrease of the

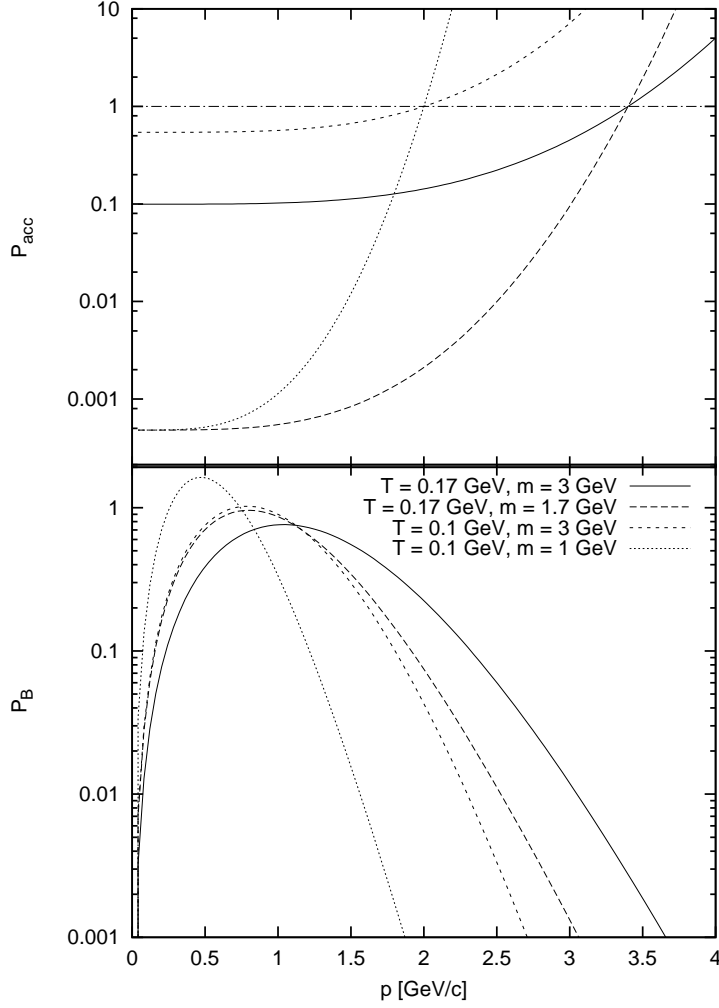


Fig. A.2. Top: The acceptance probability for heavy hadrons for some combinations of mass and temperature calculated according to eq. (A.6). Bottom: Boltzmann distribution of momenta for heavy hadrons.

non-relativistic distribution. The parameter A must be chosen. If it is small, then as a result the algorithm will produce too few hadrons with momenta above AT . On the other hand, if A is too large, then the acceptance probability will become very small at small momenta and the algorithm becomes ineffective or even not working. For usual freeze-out temperatures, between say 100 and 180 MeV, the default reasonable setting is $A = 20$. For this choice, in case $T = 0.1$ GeV and $m = 3$ GeV/ c the fraction of hadrons which is suppressed due to this artifact is at the level 0.86%. Increasing temperature and decreasing the mass makes this fraction yet smaller. On the other hand if this algorithm is used for masses larger than $10T$, then minimum acceptance probability is reached for the smallest mass $10T$ and $p = 0$ and is about $4.8 \cdot 10^{-4}$. In Figure A.2 the acceptance probabilities as functions of momentum for heavy (non-relativistic) hadrons are shown.

References

- [1] Y. Aoki, G. Endrodi, Z. Fodor, S. D. Katz and K. K. Szabo, *Nature* **443** (2006) 675 [arXiv:hep-lat/0611014].
- [2] Z. Fodor and S. D. Katz, *JHEP* **0404** (2004) 050 [arXiv:hep-lat/0402006].
- [3] P. de Forcrand and O. Philipsen, *Nucl. Phys. B* **673** (2003) 170 [arXiv:hep-lat/0307020].
- [4] C. R. Allton, S. Ejiri, S. J. Hands, O. Kaczmarek, F. Karsch, E. Laermann and C. Schmidt, *Phys. Rev. D* **68** (2003) 014507 [arXiv:hep-lat/0305007].
- [5] I. N. Mishustin, *Phys. Rev. Lett.* **82** (1999) 4779 [arXiv:hep-ph/9811307].
- [6] O. Scavenius, A. Dumitru, E. S. Fraga, J. T. Lenaghan and A. D. Jackson, *Phys. Rev. D* **63** (2001) 116003 [arXiv:hep-ph/0009171].
- [7] P. Chomaz, M. Colonna and J. Randrup, *Phys. Rept.* **389** (2004) 263.
- [8] G. Torrieri, B. Tomášik and I. Mishustin, *Phys. Rev. C* **77** (2008) 034903 [arXiv:0707.4405 [nucl-th]].
- [9] G. Torrieri and I. Mishustin, *Phys. Rev. C* **78** (2008) 021901 [arXiv:0805.0442 [hep-ph]].
- [10] T. Csörgő and B. Lörstad, *Phys. Rev. C* **54** (1996) 1390 [arXiv:hep-ph/9509213].
- [11] M. Csanád, T. Csörgő and B. Lörstad, *Nucl. Phys. A* **742** (2004) 80 [arXiv:nucl-th/0310040].
- [12] B. Tomášik, U. A. Wiedemann and U. W. Heinz, *Heavy Ion Phys.* **17** (2003) 105 [arXiv:nucl-th/9907096].
- [13] F. Retière and M. A. Lisa, *Phys. Rev. C* **70** (2004) 044907 [arXiv:nucl-th/0312024].
- [14] W. Broniowski and W. Florkowski, *Phys. Rev. Lett.* **87** (2001) 272302 [arXiv:nucl-th/0106050].
- [15] G. Torrieri, S. Steinke, W. Broniowski, W. Florkowski, J. Letessier and J. Rafelski, *Comput. Phys. Commun.* **167** (2005) 229 [arXiv:nucl-th/0404083].
- [16] J. Cleymans, H. Oeschler, K. Redlich and S. Wheaton, *Phys. Rev. C* **73** (2006) 034905 [arXiv:hep-ph/0511094].
- [17] P. Braun-Munzinger, D. Magestro, K. Redlich and J. Stachel, *Phys. Lett. B* **518** (2001) 41 [arXiv:hep-ph/0105229].
- [18] F. Becattini, M. Gaździcki, A. Keränen, J. Manninen and R. Stock, *Phys. Rev. C* **69** (2004) 024905 [arXiv:hep-ph/0310049].
- [19] K. Adcox *et al.* [PHENIX Collaboration], *Phys. Rev. C* **66** (2002) 024901 [arXiv:nucl-ex/0203015].

- [20] J. Adams *et al.* [STAR Collaboration], Phys. Rev. C **71** (2005) 064906 [arXiv:nucl-ex/0308033].
- [21] W. Broniowski, B. Hiller, W. Florkowski and P. Bożek, Phys. Lett. B **635** (2006) 290 [arXiv:nucl-th/0510033].
- [22] W. Li [PHOBOS Collaboration], PoS C **FRNC2006** (2006) 006.
- [23] A. Kisiel, T. Tałuć, W. Broniowski and W. Florkowski, Comput. Phys. Commun. **174** (2006) 669 [arXiv:nucl-th/0504047].
- [24] <http://www.cunuke.phys.columbia.edu/OSCAR/>
- [25] B. Tomášik, Acta Phys. Polon. B **36** (2005) 2087 [arXiv:nucl-th/0409074].
- [26] I. N. Mishustin, arXiv:hep-ph/0512366.
- [27] W.-M. Yao *et al.*, Journal of Physics, G **33** (2006) 1.
- [28] A. Kisiel, W. Florkowski and W. Broniowski, Phys. Rev. C **73** (2006) 064902 [arXiv:nucl-th/0602039].
- [29] G. Torrieri, S. Jeon, J. Letessier and J. Rafelski, Comput. Phys. Commun. **175** (2006) 635 [arXiv:nucl-th/0603026].
- [30] C. Adler *et al.* [STAR Collaboration], Phys. Rev. Lett. **87** (2001) 182301 [arXiv:nucl-ex/0107003].
- [31] W.H. Press, B.P. Flannery, S.A. Teukolsky, W.T. Vetterling, *Numerical recipes in C*, Cambridge University Press, 1992.